DOI: https://doi.org/10.24425/amm.2025.154479

Ł. ROGAL®¹*, Z. KOBYLARZ¹, M. GODLEWSKI¹, P. KLIMCZYK®², M. PODSIADŁO®², J. KASPRZYCKI®¹, G. GARZEL®¹, A. JARZEMBSKA®¹, M. SZCZERBA®¹, M. SZLEZYNGER¹, L. LITYŃSKA-DOBRZYNSKA®¹, L. DEMBINSKI³, A. SYPIEѹ, J. DUTKIEWICZ®¹*

CRYSTALLIZATION OF CUZrAGAI BULK METALLIC GLASS AT VARIOUS TEMPERATURES AND PRESSURES

The Cu₄₃Zr₄₃Ag₇Al₇ alloy was obtained in an amorphous form through inert gas spray forming, followed by separation using a tower cyclone gas separator. The resulting spherical particles in size of 11 µm. The consolidation of the powder was carried out using two distinct methods. First, Spark Plasma Sintering (SPS) was performed under a pressure of 35 MPa at two temperatures: 750°C and 900°C. Second, the High-Pressure High-Temperature (HPHT) method was applied, utilizing a toroidal-type Bridgman apparatus at about 560°C under a pressure of 7.8 GPa. In both processes, the consolidation duration was one minute. Differential scanning calorimetry (DSC), X-ray diffraction (XRD), and high-resolution transmission electron microscopy (HRTEM) analyses revealed distinct differences in the crystallization behavior of the alloy. SPS processing led to complete crystallization, resulting in the formation of Zr₂Cu, Ag₂Al, and Cu₁₀Zr₇ crystalline phases. In contrast, the HPHT method significantly delayed crystallization, with only nano-crystalline nuclei observed within the amorphous matrix. Additionally, the application of high pressure in the HPHT process resulted in lower porosity and higher hardness compared to the SPS method.

Keywords: Zr base amorphous alloys; high-pressure consolidation; short-range ordering; nanocrystallization of glass

1. Introduction

Zirconium-based bulk metallic glasses (BMGs) are characterized by high strength, large elastic strain, and a low Young's modulus, making them attractive for various industrial applications [1]. However, BMGs are inherently metastable and can crystallize into a stable structure when subjected to thermal variations [2,3]. When metallic glasses are heated above their glass transition temperature (T_g) or crystallization temperature (T_x) , their amorphous structure transforms into crystalline phases [1,2]. The nucleation and growth of these phases depend on several factors, including heating rate, duration, and pressure. In this study, a Cu-Zr-Ag-Al amorphous alloy was selected due to its excellent glass-forming ability, which allows for the production of an amorphous powder at a relatively low critical cooling rate. Specifically, the critical cooling rate (Rc) of Cu₄₂Zr₄₂Ag₈Al₈ is only 4°C/s [4], whereas Zr₄₈Zr₄₈Al₄ requires nearly 40°C/s [5], and CuZr demands an even higher rate of 250°C/s [5]. The crystallization of glassy alloys typically leads to the formation of complex intermetallic compounds, such as ZrCu and Zr₂Cu, which significantly influence the material's

mechanical properties [6-8]. Previous studies have explored the crystallization behavior of Zr-based metallic glasses. Yokoyama et al. [9] investigated Zr–Cu–Al ternary alloys, identifying three intermetallic compounds – ZrCu, Zr₂Cu, and Zr₇Cu₁₀. The ZrCu phase, with a B2 structure, remains stable above 715°C but decomposes into Zr₂Cu (C11b structure) and Zr₇Cu₁₀ upon cooling. Additionally, the B2-ordered ZrCu phase undergoes a martensitic phase transformation. However, reports on the precipitation of the ZrCu-B2 phase in rapidly quenched Zr–Cu binary and Zr–Cu–Al ternary alloys remain scarce. More recently, Zhang et al. [2,3] observed significant precipitation of the ZrCu-B2 phase in Zr₅₀Cu₄₀Al₁₀ (at.%) BMGs produced via tilt casting and subjected to rapid heating, confirming that the ZrCu phase remains stable at room temperature. They attributed this phenomenon to long-range diffusion and elastic strain energy.

Applying hydrostatic high pressure during sintering significantly affects crystallization behavior by reducing atomic mobility [2,10-12]. Studies have reported a notable increase in T_x under high pressure, reaching 9.4 K/GPa in ZrAlNiCuAg alloys [13] and 12.8 K/GPa in ZrCuTiNiBe alloys at pressures of 4-6 GPa [14]. This effect has been linked to the shortening of

^{*} Corresponding author: l.rogal@imim.pl, j.dutkiewicz@imim.pl



INSTITUTE OF METALLURGY AND MATERIALS SCIENCE POLISH ACADEMY OF SCIENCE, 25 REYMONTA STR., 30-059 KRAKOW, POLAND

² ŁUKASIEWICZ RESEARCH NETWORK, KRAKOW INSTITUTE OF TECHNOLOGY, KRAKOW, POLANI

³ SITE UTBM, DÉPARTEMENT ICB-CO2M, BELFORT CEDEX, FRANCE

Zr–Zr bonds, which alters atomic packing in Zr₅₀Cu₅₀ metallic glasses under high pressure. Additionally, high pressure induces atomic composition segregation, as Zr-Zr and Cu-Cu bonds contract more readily than Zr-Cu bonds, leading to changes in structural stability [2,3,6,8]. Dmowski et al. [2] examined the high-pressure quenching of Zr-Cu-Al-Pd metallic glasses from the supercooled liquid state and found that their structure differed from glasses quenched without pressure. Interestingly, the high-pressure-induced structure reverted to its original form upon annealing without pressure. Fully amorphous compacts, sintered at temperatures above Tg, reached a compression strength of 1174 MPa. As shown in [11], at pressures exceeding 8 GPa, Zr-based metallic glasses heated to the supercooled liquid state remained amorphous. In Zr-Ti-Cu-Ni-Be metallic glasses, crystallization temperature increases within the pressure range of ~4.5 GPa, attributed to pressure-induced suppression of atomic mobility [3,6-14]. This phenomenon is linked to a reduction in free volume within the glassy phase, leading to increased density and retarded crystallization [10-16]. Considering previous studies on the high-pressure modification of amorphous structures, both from theoretical calculations [6-11] and experimental investigations [2,3,6-16], some discrepancies remain regarding the effects of high pressure on T_g and T_x , as well as the underlying mechanisms of amorphization and crystallization. Notably, nano-crystallization has been observed within the amorphous matrix under high-pressure conditions. To further investigate this phenomenon, the present study applied a short annealing time above T_x to evaluate its effects. Additionally, Spark Plasma Sintering (SPS) at 35 MPa was performed at the same temperature to assess the impact of pressure on crystallization behavior.

2. Experimental procedure

Amorphous powder $Cu_{43}Zr_{43}Ag_7Al_7$ alloy (all in at.%) was prepared using installation at the University of Belfort consisting of an autoclave head, a spray tower, a gas distribution system, and an inert gas system (cyclone separator). In the autoclave head, the insulated crucible is heated by an induction coil and the special atomizing unit, mainly the Laval nozzle and the melt nozzle. The sprayed liquid metal in the spherical form was cooled relatively quickly as it fell, rotating in the tower. X-ray diffraction and DSC studies confirmed its amorphous structure. Fig. 1 shows an SEM micrograph of the powder and its size distribution, indicating the average size of spheres near $11 \pm 9~\mu m$.

For the investigated alloy, sintering temperatures of 750°C and 900°C were chosen for 1 minute to study the effect of short-term temperature impact on the microstructure and to obtain good-quality sintered samples at pressures of 35 MPa for the SPS (Spark Plasma Sintering) and at about 560°C for 1 min at 7.8 GPa using a toroidal-type Bridgeman apparatus (High-Pressure High Temperature). The temperature during synthesis was not measured directly on the sample. The device had been previously calibrated, and the generator was operated at the appropriate power level to ensure the required temperature.

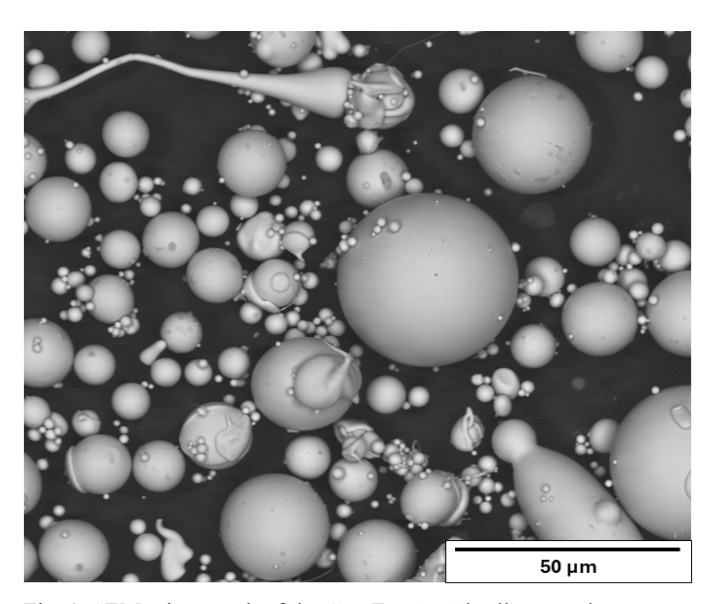


Fig. 1. SEM micrograph of the Cu₄₃Zr₄₃Ag₇Al₇ alloy powder

The X-ray measurements of the phase composition were performed using a D2 Phaser-Bruker diffractometer with Cu-Ka filtered radiation. The microstructure was examined using a scanning electron microscope FEI SEM XL30 (FEI Company, Hillsboro, OR) equipped with an energy-dispersive X-ray spectrometer EDAX GEMINI 4000. The microstructure and selected area electron diffraction pattern (SAEDP) studies were performed using a Tecnai G2 F20 transmission electron microscope (TEM). Thin foils for TEM were prepared using an FEI Quanta 3D 200 Dual Beam Focused Ion Beam (FIB) equipped with an Omniprobe lift-out system. The glass transition temperatures and crystallization temperature were studied using the F1 404 Netzsch. The recovered samples, after sintering, were heated at the rate of 20°C/min in an argon atmosphere. The Vickers hardness was measured under a load of 0,05 kg using an Innovatest microhardness tester.

3. Results and discussion

In the first step, gas-atomized Zr-based amorphous powders with T_x temperature of 497°C were consolidated. Fig. 2 shows X-ray diffraction curves from the samples sintered using the SPS method at 750°C and 900°C (two upper patterns), while the lowest one shows the diffraction curve from the alloy sintered at 7.8 GPa/560°C. Samples obtained using the SPS method show similar diffraction patterns with frequent maxima from the crystalline phases identified as Zr₂Cu, Ag₂Al, and Cu₁₀Zr₇. It indicates almost complete crystallization after sintering using the SPS method above the T_r temperature. The sample sintered at 560°C at 7.8 GPa shows a fully amorphous structure, confirming that annealing at 560°C by simultaneities high-pressure delays the crystallization of amorphous structure. Most of the studies presented in the literature concern sintering below T_r temperature. A fully glassy structure has been obtained in Zr-Cu-Y-Al compacts with a high density manufactured by SPS at 390°C

and a pressure of 35 MPa, attaining hardness 396 HV $_{0.3}$ [16]. Sintering at higher temperatures involved crystallization of the sample. Temperatures below the crystallization temperature were also used to consolidate the ball-milled Zr–Cu–Al and Zr-Ni–Ti–Cu amorphous powders using high pressure of 4-7 GPa. Sintering temperature was applied below T_x , and good quality amorphous compacts strengthened by nanocrystalline inclusions were obtained with a hardness of 1224 HV, i.e., higher than reported for the SPS consolidated samples [16,17].

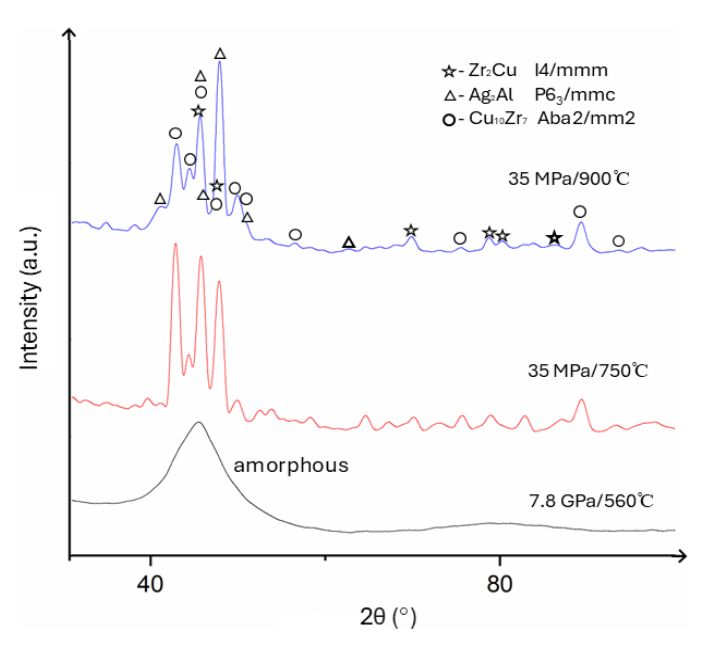


Fig. 2. X-ray diffraction pattern of the $\rm Cu_{43}Zr_{43}Ag_7Al_7$ alloy prepared by the SPS method at 750°C and 900°C (upper curves) and high pressure 7.8 GPa/900°C sintering

Fig. 3 shows DSC curves obtained during continuous heating of the $Cu_{43}Zr_{43}Ag_7Al_7$ glass powder after sintering using the SPS method at 750°C and 900°C and a high-pressure technique at 7.8 GPa at 560°C. One can see that, similarly to the X-ray dif-

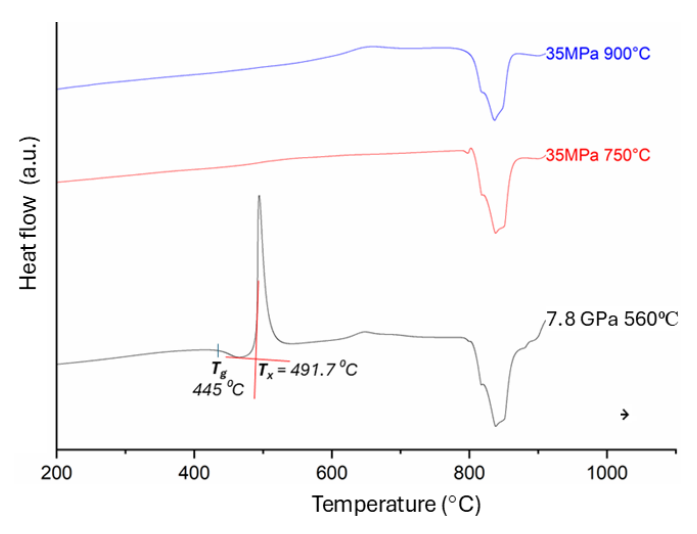
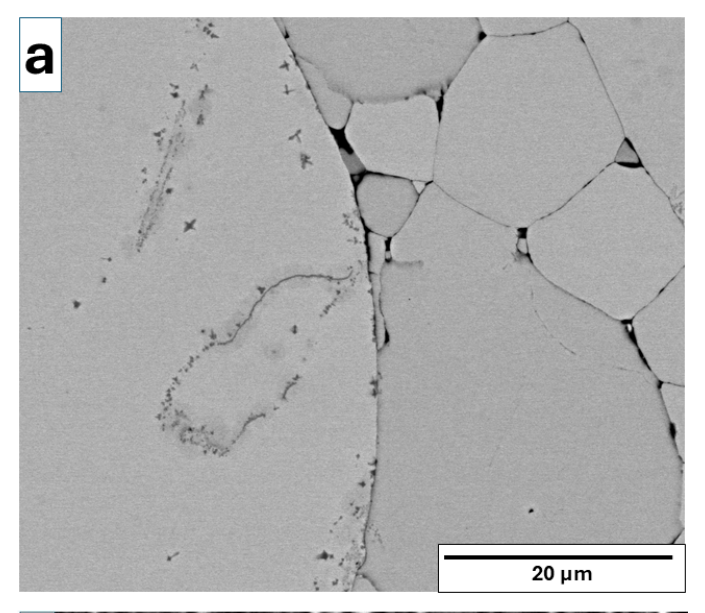


Fig. 3. DSC curves taken during continuous heating of the as-prepared powder, samples sintered by the SPS method at 750°C and 900°C and a high-pressure method at 7.8 GPa/560°C

fraction study, the SPS method resulted in the complete crystallization of powders. At the same time, high pressure did not cause visible crystallization effects despite 5.3°C degrees shift of the T_x temperature (491.7°C) to lower temperatures. It is probably caused by an easier nucleation of the crystalline phase using ordered nuclei formed during 560°C sintering ($T_x = 497$ °C). It indicates that a pressure of 7.8 GPa delays the crystallization at high pressure due to slow-down diffusion.

Fig. 4 shows microstructures from the alloy sintered using high pressure of 7.8 GPa at 560°C. SEM micrograph (Fig. 4a) revealed a few fine precipitates at the grain boundaries, indicating the beginning of the crystallization process from the area with the highest energy. The majority of the sample area does not show any precipitates. In the HRTEM micrograph in Fig. 4b, the sample shows a random distribution of atoms; however, in some places (marked by white circles), one can distinguish ordered atomic structures of the size of a few interatomic distances resem-



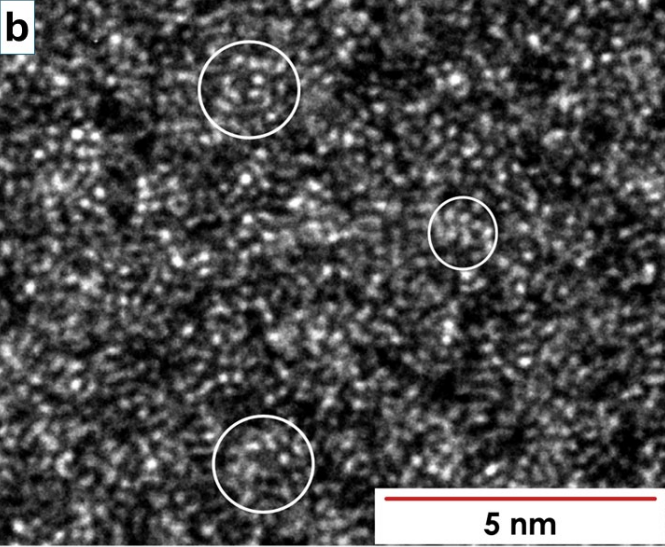
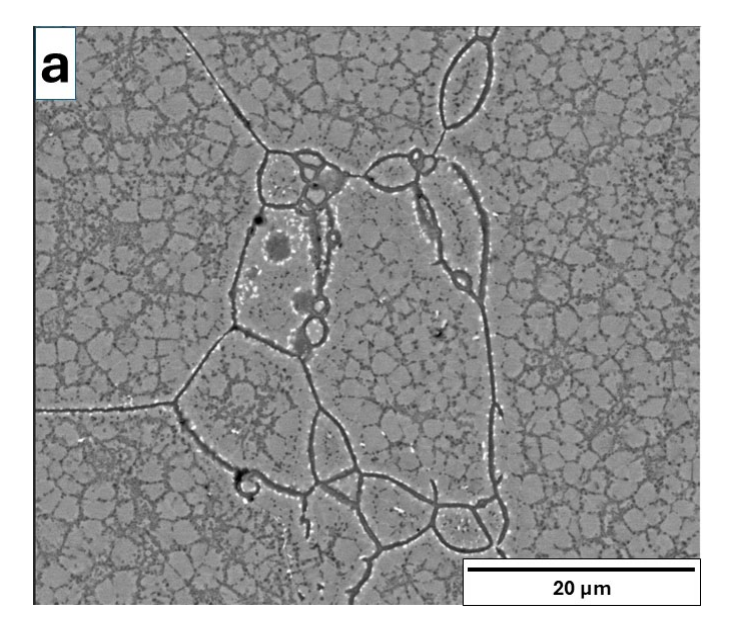
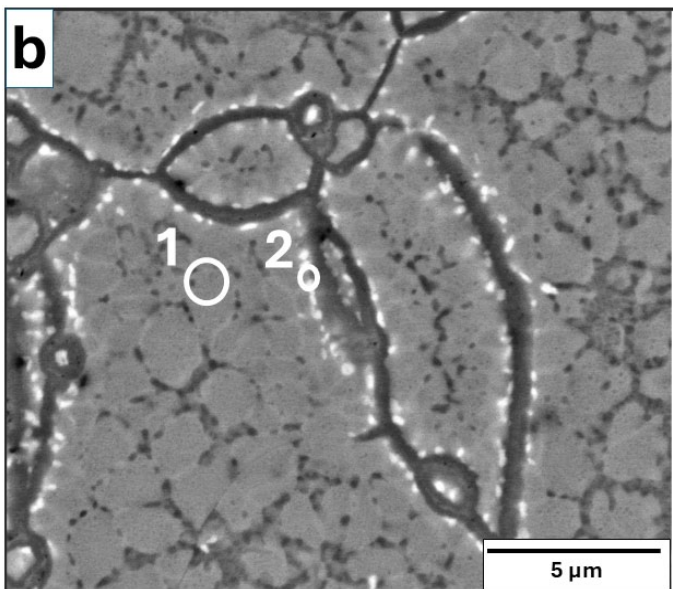


Fig. 4. $Cu_{43}Zr_{43}Ag_7Al_7$ alloy sintered under high pressure of 7.8 GPa at about 560°C; a) SEM micrograph showing fine precipitates along the grain boundaries, and b) HRTEM image illustrating a mainly random distribution of atoms with a few marked regions of ordered atomic structure





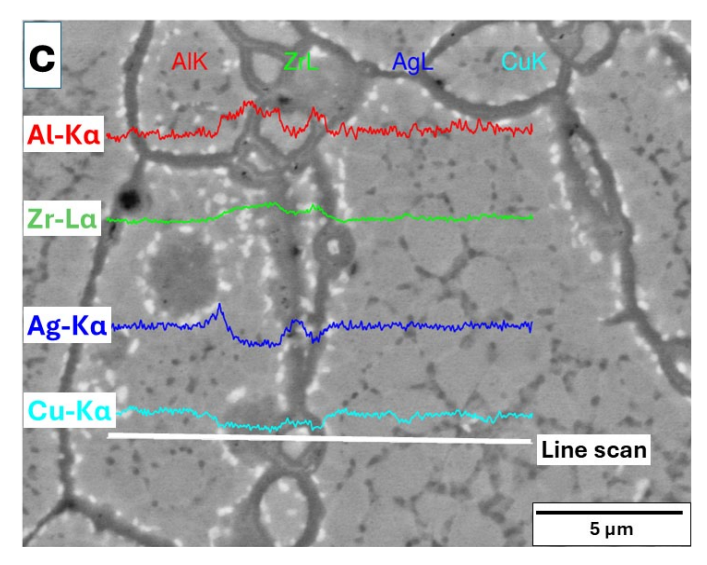


Fig. 5. a) SEM micrograph of the SPS sintered sample at 750° C using the SPS method, b) with EDS analysis points marked on the white precipitates and matrix (the results of the chemical analysis are presented in TABLE 1), c) Line scan composition change of characteristic radiation measurement Al K, Zr L, Ag K, Cu K

bling the atomic positions in a crystalline plane. They are a few nm in size with an inter-plane distance of a densely packed plane. It indicates most probably the beginning of the atomic ordering process, as Dmowski [2] observed in alloys heated under high pressure. The SEM-BSE results of the SPS sample sintered at 750°C with chemical analysis are shown in Fig. 5. The microstructure consists of fully crystallized grains with an average size of $72 \pm 26 \,\mu m$ within the smaller one with 2-4 μm diameter visible. They are formed most probably discontinuously and have an overall alloy composition (point 1 in Fig. 5, TABLE 1). Around small grains, clear dark broadened boundaries, and fine bright precipitates (size near 0,1 µm) are visible. Combined points and line scan EDS chemical analysis confirmed segregation of Al and Zr to boundaries and Ag to white precipitations (point 2, Fig. 5, TABLE 1 and line scan Fig. 5b). Previous studies suggest that Cu₁₀Zr₇ and the Zr₂Cu + AlCu₂Zr eutectic phases are reported to be formed from the melt [20,21]. The aged amorphous alloys show nanocrystals formed during annealing [20] similar phases to that observed in dynamically loaded ZrCuAgAl amorphous alloys [21] (i.e., AlCu₂Zr, Al₂Zr, and AgZr). Summarizing microanalysis results suggests the presence of previously observed AgZr, Cu₁₀Zr₇, and possibly Cu₂ZrAl.

The results of SEM-BSE studies of the SPS sample at 900°C are shown in Fig. 6. Stronger segregation in the matrix is visible (point 1, Fig. 6, TABLE 1) compared to the sample processed at 750°C. The precipitates are larger and show better signals for chemical analysis. However, their distribution is different; bright fine precipitates are distributed along lines inside the grains, while dark oval precipitates are distributed randomly inside the grains. Dark precipitates are rich in copper and contain less zirconium (point 2, Fig. 6, TABLE 1), and they can be attached to $Cu_{10}Zr_7$ with Al and Ag substituting Cu and Zr. However, the presence of Cu_2ZrAl is observed in ref. [22] cannot be excluded. $Cu_{10}Zr_7$ precipitates were identified in the analysis of the electron

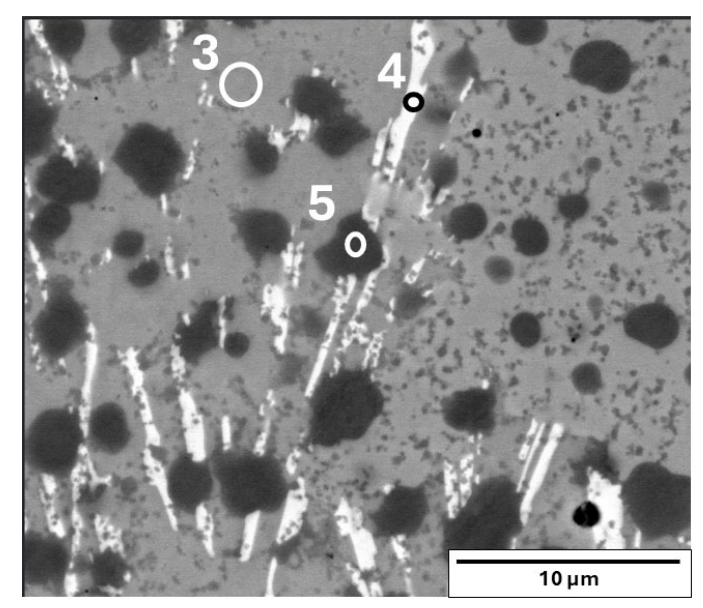


Fig. 6. SEM micrograph of the SPS sintered sample at 900°C using the SPS method, with EDS analysis points marked on the precipitates and matrix. The results of the chemical analysis are presented in TABLE 1

EDS chemical analysis results of sintered at 750 and 900°C using the SPS method samples from areas marked in Figs. 5 and 6

Place of analysis	Place of analysis	Element [%at.]			
		Zr	Cu	Ag	Al
SEM EDS Fig. 5	1 – grey matrix area	$42,0 \pm 0,8$	$44,2 \pm 0,9$	$7,2 \pm 0,3$	$6,6 \pm 0,3$
	2 – bright precipitation	43.8 ± 1.0	$38,3 \pm 0,8$	$13,3 \pm 0,5$	$4,6 \pm 0,9$
SEM EDS Fig. 6	3 – grey matrix area	47.8 ± 1.0	$44,2 \pm 0,9$	$4,7 \pm 0,9$	$3,3 \pm 0,6$
	2 – bright precipitation	$46,5 \pm 0,9$	$28,8 \pm 0,6$	$22,5 \pm 0,5$	$2,2 \pm 0,4$
	3 – dark precipitation	$30,1 \pm 0,6$	$49,1 \pm 1,0$	$6,4 \pm 0,3$	$14,4 \pm 0,6$

diffraction pattern (Fig. 2), which strengthens such interpretation. Bright particles formed along lines contain more Zr and Ag and less Cu and almost no Al (point 3, Fig. 6, TABLE 1). Therefore, this phase can be identified as ZrAg (in accordance with ref. [22], where Cu can substitute Ag. Finally, the grey phase containing less aluminum than the other phases can be identified as Zr₂Cu or CuZr phase with Al and Ag substituting Cu and Zr. The presence of Ag₂Al was not confirmed by microanalysis of SPS compacted alloys.

To illustrate the crystallization of glass, a qualitative chemical analysis was conducted using EDS in SEM to determine the distribution of elements. The matrix was confirmed to consist of relatively homogeneously distributed Zr, Cu, Al, and Ag (Fig. 7). Within it, there is a strong segregation of phases containing Cu and Al as well as Ag-enriched phases.

The HPHT-sintered alloy exhibited a hardness of 722 ± 25 HV. In contrast, the SPS-sintered samples demonstrated lower hardness values of 670 ± 28 HV and 524 ± 33 HV at 750° C and 900° C, respectively. These results align with previous findings on high-pressure consolidated ZrCuAl and ZrNiTiCu alloys [19,22]. The higher hardness observed in samples undergoing early-stage precipitation is consistent with crystallization studies of CuZrAlAg alloys [21,22], where partially crystallized samples exhibited greater hardness than both fully crystallized and initial

amorphous states. Furthermore, the early-stage precipitation of the ZrAg phase supports the findings of [23], suggesting that ZrAg precipitation competes with B2 ZrCu crystallization, thereby enhancing the glass-forming ability of CuZrAgAl alloys.

4. Conclusions

- SPS consolidation at 35 MPa and temperatures above the T_x temperature (750-900°C) allowed obtaining a good-quality consolidated sample with a fully transformed crystalline structure. TEM and SEM studies suggested the presence of Cu₁₀Zr₇, ZrAg, Cu₂ZrAl, and Zr₂Cu intermetallic phases with other elements partially substituting the components of the compound.
- 2. The high pressure of 7,8 GPa sintering caused a significant delay of crystallization during sintering at 560°C due to a high-intensity crystallization peak in the DSC measurement. The sintered samples showed a few discontinuous particles near grain boundaries due to fine precipitation of the ZrAl and ZrAg phases. HRTEM allowed the identification of atomic planes within fine nanometer-size particles, indicating short-range order nuclei affecting the crystallization temperature of the sintered sample.

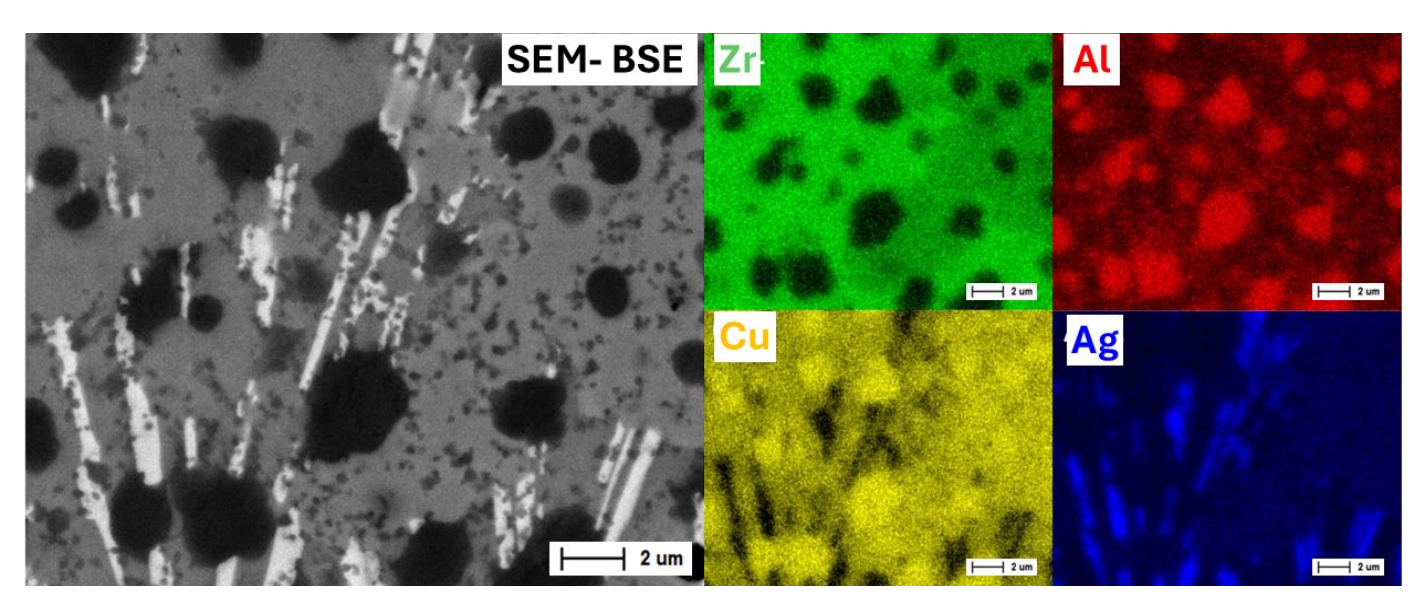


Fig. 7. SEM image of the SPS sintered sample at 900°C with mapping area frames of EDS analysis points (a) and surface distributions of alloy constituents: Zr, Cu, Al, Ag

Acknowledgments

This work was financed by the National Science Centre, Poland, project No. UMO-2022/47/B/ST8/03153 entitled: Tailoring properties and structure of Mg- and Zr-based metallic glasses by ultra-high pressure. The results were presented during 14th Polish Japanese Joint Seminar on Micro and Nano Analysis (3-6.09.2024, Toyama, Japan). The financial support of Polish Academy of Sciences is greatly appreciated.

REFERENCES

- [1] C. Suryanarayana, A. Inoue, Bulk metallic Glasses, Taylor & Francis Group, 342 (2011).
- W. Dmowski, S. Gierlotka, Z. Wang, Y. Yokoyama, B. Palosz, [2] T. Egami, Pressure Induced Liquid-to-Liquid Transition in Zrbased Supercooled Melts and Pressure Quenched Glasses, Scientific Reports, 6564 (2017).
- [3] Hong-Wei Zhang, T.J. Zhou, Pressure effect on the crystallization behavior of Zr46.7Ti8.3Cu7.5Ni10Be27.5 bulk metallic glass. Physics Letters, 297-301 (2006).
- Q.S. Zhang, W. Zhang, A. Inoue, New Cu-Zr base bulk metallic glasses with large diameters up to 1,5 cm. Scr. Mater. 55, 711-713
- [5] W.H. Wang, J. Lewandowski, A.L. Greer, Understanding the glass forming ability of Cu50Zr50 alloy in terms of a metastable eutectic. J. Mater. Res. 19, 2307-2013 (2004).
- Yong Yong Wang, Xiao Dong, Xiaohui Song, Xue Ping Li, Gong Li, The effect of composition on pressure-induced polyamorphism in metallic glasses. Materials Letters, 142-145 (2017).
- [7] Heng Kang, Xin Ye, Ji Wang, Shaopeng Pan, Limin Wang, Abnormal bonding ways in Zr50Cu50 metallic glass under high pressures. J. Alloys Comp., 512-517 (2019).
- P. Dziegielewski, Georgos Evangelakis, Jerzy Antonowicz, Shortto-medium range atomic order of Zr-Cu metallic glasses under compression. Computational Materials Science, 111345 (2022).
- Y. Yokoyama, H. Fredriksson, H. Yasuda, M. Nishijima, A. Inoue, Glassy solidification criterion of Zr 50Cu40Al10 alloy. Mater. Trans. 48, 1363 (2007).
- [10] P.F. Wang, C.X. Peng, Y. Cheng, L.J. Jia, Y.Y. Wang, L. Wang, Atomic structure evolution of (CuZr)100-xAgx glass under compression deformation. Journal of Alloys and Compounds, 44-51 (2019).
- [11] M. Celtek, S. Sengul, U. Domekeli, Glass formation and structural properties of Zr50Cu50-xAlx bulk metallic glasses investigated by molecular dynamics simulations. Intermetallics, 62-73 (2017).

- [12] W. H. Wang, P. Wen, D. Q. Zhao, M. X. Pan, T. Okada, W. Utsumi, Nucleation and growth in bulk metallic glass under high pressure investigated using in situ x-ray diffraction Appl. Phys. Lett., 5202-5204 (2003).
- [13] Jia Zhang, Hai Feng Zhang, Ming Xiu Quan, Zhuang Qi Hu, Effect of pressure on crystallization process of Zr55Al10Ni5Cu30 bulk metallic glass. Materials Letters, 1379-1382 (2004).
- [14] J.S. Jiang Y.X. Zhuang, H. Rasmussen, J. Saida and A. Inoue formation of quasicrystals and amorphous to quasicrystalline phase transformation kinetics in Zr₆₅Al_{7.5}Al₁₀Cu_{7.5}Ag₁₀ metallic glass under pressure. Phys. Rev. B 64, 094208-1-094208-10 (2001).
- [15] C. Yang, W.K. Wang, R.P. Liu, Z.J. Zhan, L.L. Sun, J. Zhang, J.Z. Jiang, L. Yang, C. Lathe, Crystallization of Zr41Ti14Cu12.5Cu10Ni10Be22.5 bulk metallic glass under high pressure examined by in-situ synchrotronradiation X-ray diffraction. J. Appl. Phys. 99, 023525-1-023525-4 (2006).
- [16] Qifan Wang, Hongbo Lou, Yoshio Kono, Daijo Ikuta, Zhidan Zeng, Qiaoshi Zeng, Viscosity anomaly of a metallic glass-forming liquid under high pressure. J. Non-Cryst. Solids, 122412 (2023).
- [17] H. Cai, G. Zhou, P.W. Li, D.W. Ding, Q. An, Yixian Li, Q. Yang, H. Mao, Mechanical, wetting and corrosion properties of a Zrbased amorphous alloy composite consolidated by spark plasma sintering. J. Non-Cryst. Solids, 122648 (2023).
- [18] M. Suarez, D. Fernandez-Gonzalez, L.A. Díaz, F. Diologent, L.F. Verdeja, A. Fernandez, Consolidation and mechanical properties of ZrCu_{39,85}Y_{2,37}Al_{1,8} bulk metallic glass obtained from gas-atomized powders by spark plasma sintering. Intermetallics, 107366 (2021).
- [19] J. Dutkiewicz, L. Jaworska, W. Maziarz, T. Czeppe, M. Lejkowska, M. Kubicek, M. Pastrnak, Consolidation of amorphous ball-milled Zr-Cu-Al and Zr-Ni-Ti-Cu powders,. J. Alloys Comp., 333-335 (2007).
- [20] Q.S. Zhang, W. Zhang, G.Q. Xie, A. Inoue, Eutectic crystallization behavior of new Zr48Cu36Al8Ag8 alloy with high glass-forming ability. J. Phys. Conf. Ser. 144, 012031 (2009).
- [21] Y. Liu, J.J. Blandin, M. Suery, G. Kapelski, Effect of cooling rate on the microstructure and microhardness of the CuZrAgAl alloy, Mater. Charact., 8-13 (2012).
- [22] Christoph Gammer, Christian Rentenberger, Denise Beitelschmidt, Andrew M. Minor, Jürgen Eckert, Direct observation of nanocrystal-induced enhancement of tensile ductility in a metallic glass composite, Materials & Design, 109970 (2021).
- [23] C. Gammer, B. Escher, C. Ebner, A. M. Minor, H. P. Karnthaler, J. Eckert, S. Pauly, C. Rentenberger, Influence of the Ag concentration on the medium-range order in a CuZrAlAg bulk metallic glass, Scientific Reports | 7:44903 |

DOI: https://doi.org/10.1038/srep44903